Flow Measurement and Instrumentation 85 (2022) 102170

Contents lists available at ScienceDirect

Flow Measurement and Instrumentation

journal homepage: www.elsevier.com/locate/flowmeasinst

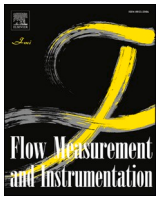

Hydraulic characterization of a second-generation common rail injector operating under solo and split injection strategies

Vu H. Nguyen [a], Andrea Cavicchi [b], Dat X. Nguyen [a], Kien T. Nguyen [a], Phuong X. Pham [a,*], Lucio Postrioti [b]

[a] Faculty of Vehicle and Energy Engineering - Le Quy Don Technical University, Viet Nam
[b] Dipartimento di Ingegneria, Università di Perugia, Italy

ARTICLE INFO

Keywords:
Hydraulic characterization
Split injection
Second-generation common rail injector

ABSTRACT

In modern compression ignition engines, complex fuel injection strategies are adopted in order to enable a clean and efficient combustion process and an effective combustion noise control algorithm. Multi-injection strategies inject fuel into the combustion chamber several times (e.g. pilot, main, and post injections) during each combustion cycle, while split-injection approach further divides the main injection into different shots, with very short dwell time. Split injection may help to enhance air entrainment into the spray core where the fuel droplets are highly dense and mixing quality is poor. These advanced injection techniques lead to complex hydraulic behaviors including injection instability and eventually affecting fuel metering accuracy, hence detailed investigations are required. Understanding hydraulic characteristics especially during peculiar events like start/end of injection and accurately quantifying the actual injection volume, injection rate, and pressure variations in different locations of the injection system in each single activation of a complex strategy are key targets. In this work, the hydraulic behavior of a second generation common-rail solenoid injector operating under split-injection strategy has been experimentally investigated in terms of injection rate and injected volume. An extensive experiment has been conducted in this study using a state-of-the-art injection system operating on a hydraulic test bench equipped with a Zeuch-method type injection analyzer. It is found that although the standard of deviation of injection rates and injected volume is quite small for isolated injection events, the shot-to-shot deviation for split-injection mode can be significantly higher depending mainly on dwell time, fuel quantity ratio between the two shots and injection pressure level, as an effect of both pressure perturbations in the feeding line and in the injector caused by close actuations, eventually joined to inertial phenomena of the injector needle. The present paper reports an analysis methodology for the quantitative evaluation of systematic inter-cycle deviations, in the effort towards a deeper exploitation of the potential benefits offered by advanced injection strategies.

1. Introduction

Hydraulic characteristics including injection instability in the fuel system of internal combustion engines correlate well with important injection parameters; therefore, it is critically important to characterize the hydraulic behaviors to (i) control the injection process, especially advanced injection technique including multi-injection and split injection, (ii) to ensure fuel supply into a cylinder in a right time and right amount, (iii) improve air/fuel mixing and combustion efficiency, and (iv) decrease engine noise and exhaust emission [1,2]. However, quantifying the hydraulic system's parameters is always challenging due to high frequency of the injector, the equivalent sound speed pressure wave in the fuel system during the injection, and the randomness of the injection process [3]. For example, quantifying the actual hydraulic start of injection (SOI) could be done by using energizing pulse, fuel rail pressure, and injector needle lift. Common methods used in the literature are to adopt one of those signals. However, the evidences representing the SOI event could be different from one signal to the others. This is due to hydraulic, mechanical, and electric lags in the injection system. The time lags make the injection timings, obtained from different signals throughout the current literature, inconsistent. Hydraulic characteristics are also affected by a number of boundary conditions such as pressure-time history upstream of the injector nozzle,

* Corresponding author.
E-mail address: phuongpham@lqdtu.edu.vn (P.X. Pham).

https://doi.org/10.1016/j.flowmeasinst.2022.102170
Received 15 June 2021; Received in revised form 28 March 2022; Accepted 6 April 2022
Available online 9 April 2022

Nomenclatures

Abbreviations	*Definitions*
ET	Energizing time
DT	Dwell time
IR	Injection rate
p	Pressure
p_{rail}	Nominal rail pressure
$p_{railpipe}$	Actual pressure in the common rail
P_{pipe}	Pressure in the high-pressure line
$p_{pipeRed}$	Pipe pressure reduction
p_{under}	Under-recovering pipe pressure
PCV	Pressure control valve
SCV	Suction control valve
SOE	Start of energizing
SOI	Start of injection
EOI	End of injection
SON	Start of needle lifting
NOD	Nozzle opening delay
NCD	Nozzle closing delay

back pressure, and fluid and injector temperature [4]. Quantifying the time lags and hydraulic behavior is very complex and requires a state-of-the-art technique. In the injection process, inter-cycle instability and system deviations simultaneously occur. With the advent of common rail injection systems and modern injection strategies like multi-injection and split injection, further difficulties are added to this issue. Different from multi-injection strategy in which fuel supply in one engine cycle is divided into pilot, main, and post injections, the split injection strategy investigated in this work splits the main injection into two shots. Dwell times (DT), defined as the time between the ending of one shot and the starting of the next, in the split injection mode is much shorter, while injection ratio is bigger compared to those in multi-injection mode. Under short DT and big injection ratio, hydraulic characteristics, including inter-cycle variations of split injection, are not fully investigated. Adequately detailed studies on the hydraulic characteristics, especially inter-cycle variations of common rail injection systems operating with modern injection strategies, are relatively scarce in literature, particularly for second-generation common rail injection systems. The current work will provide insights into the hydraulic behaviors of a common rail injection system operating under split injection strategy, including inter-cycle variability. Further details about multi-injection and split injection strategies will be provided lateron in this section. This work investigates (i) special events (e.g., start/end of energizing pulse, nozzle opening and closing, and start/end of fuel injection) that occur during the injection process; (ii) the characteristics of energizing pulse, injection rate, and pipe and rail pressure under solo and split injection strategies; and (iii) inter-cycle injection variability. Simultaneously measuring energizing pulse, injection rate, and pipe and rail pressure using a state-of-the-art, carefully set up and calibrated experiment system (see Section 2) allows to identify and correlate important events and features representing the hydraulic behaviors of a modern injection system operating under an advanced injection strategy.

Traditional injection methods only supply fuel once for each engine cycle. Conversely, multi-injection and split injection strategies inject fuel several times for each cycle. Multi-injection modes include pilot injections (one or more time), main injection, and post injections (one or more times). According to the authors' knowledge, the slit-injection strategy has no clear official definition. However, to differentiate multi-injection strategy from a split injection one, it can be understood that the fraction of fuel amount supplied in the pilot period or the late period to the main one does not exceed 15% [5,6]; otherwise it belongs to the split injection approach. In the split injection mode investigated in this study, the main injection is divided into different shots [7], and the volume fraction of fuel injected between the two shots is called injection ratio. DT is defined as the time from the ending of one shot to the starting of the next one. Split injection is found to be a good approach to decrease exhaust emission [8] and engine noise [9] and to improve combustion quality and engine efficiency [9,10]. The advantages mentioned above depend on injection ratio, DT, and engine operating conditions. In the split injection strategy, the influence of one shot on the next one is particularly significant for second-generation CR systems when advanced injection strategies requiring very short DTs are adopted. Certain deviations exist in the hydraulic characteristics in CR injection systems due to several physical behaviors in the systems. The main contributors to these deviations are pressure waves that developed in the rail, pipes, and injector body. The pressure waves created due to (i) injector needle opening and closing and (ii) PCV and SCV valves' activations to maintain the rail pressure and the wave developed will transfer within high-pressure pipes and rail. Those deviations should carefully be investigated to improve the quality of the fuel injection process. When adopting multi-injection and split injection strategies, the oscillation of the fuel pipe pressure created by the first shot significantly affects the hydraulic characteristics of the second shot. This leads to variations in the injection rate (IR) and total injection amount of the second shot when operating under different parameters such as DT, injection duration, injection ratio, and pressure. Carefully evaluating those variations can help to supply fuel in a right time and in a right amount, which in turn helps to improve fuel economy and decrease exhaust emission. Furthermore, the variations may significantly affect the quality of mixing, combustion, and engine performance. For example, the interactions between the latter injection with combustion products from the prior one and other parameters including ignition delays, ignition locations, and flame liftoff lengths could significantly be affected [11]. Understanding the hydraulic characteristics like pressure drop in the fuel pipe may also help to diagnose technical issues of the injection system [12].

Developing an injection system requires to address a number of complex issues, including (i) fuel metering accuracy (e.g., injection time and amount) and fuel IR [4] and (ii) determining suitable injection strategy for different engine operating conditions. A suitable injection strategy helps to improve atomization and mixing quality, leading to better combustion quality and lower exhaust pollution [13,14]. For example, split injection may help to reduce spray penetration and the wall wetting. One of the biggest issues associated with fuel–air mixing is the limitation of air entrance into the spray core where atomization may still be developing and fuel droplet density is high [14,15]. This poor oxygen entrance in the dense spray zone impairs the mixing quality in the spray core and the combustion quality. Split injection divides the main injection into several shots, and it can help to decrease the fuel particle density in the core to improve the mixing quality [10,16,17].

A work done in Ref. [18] investigates the influence of thermal conditions (fuel and injector body temperature) on hydraulic behaviors of a common rail injector operating with multi-injection strategy (solo-main, pilot-main, and main-post injection). A strong correlation was observed between thermal conditions and hydraulic behavior especially at the end of injection. In Ref. [19,31], DT and energizing time were found to have significant influence on the injection volume. Investigations into hydraulic behaviors of second-generation common rail injection systems operating with split injection strategies are quite scarce in the literature.

This current study deeply investigates special events representing hydraulic characteristics of a diesel common rail injection system such as start of energizing time, start of nozzle opening, SOI, and end of injection in a wide range of operating conditions (e.g., IR, ETs, and DTs) and inter-cycle injection variabilities. Different signals, including current pulse, IR, pipe pressure, coefficient of variations, and deviations of IRs when operating with solo/single injection and split injection modes, will simultaneously be measured and investigated. Here, split injection

is limited to double injection modes in which the main injection is divided into two consecutive shots and the influence of the first shot on the second shot is examined. This investigation may provide useful information on the time lags and hydraulic behaviors related to the injection events. This may help to provide further knowledge on the injection inter-cycle instability and to accurately control the injection timing and quantity when using split injection strategy in order to improve fuel economy and engine efficiency and decrease exhaust emission. This may also provide a good database to develop diagnosis tools using energizing pulse, pipe, and rail pressure signals.

2. Experiment setup

The injector used in this study is Bosch CRI2.2, a second-generation solenoid injector. It is an 8 × 0.144-mm hole injector and can work with injection pressure of up to 1600 bar. This injector is used in Hyundai 2.5 TCI-A engines typically equipped in medium-duty pickup vans. The hydraulic characteristics of this injector operating under solo/single injection and split injection modes are experimentally investigated thanks to a special testing system called UniPg STS (UniPG Injection Analyzer Shot-to-Shot) developed earlier at Spray Laboratory – Perugia University [20]. Based on the Zeuch approach, this system allows to simultaneously monitor current pulse, injection rate, rail pressure, and pipe pressure under traditional injection and modern injection strategies [20]. These modes are set up to be relevant with injection conditions adopted in practical engines. From these useful characteristics, important events, such as start of nozzle opening (SON), SOI, end of injection (EOI), and opening and closing delay times, will be quantified.

The UniPg STS system consists of one high-pressure pump and one fuel rail with four high-pressure pipes to connect with four injectors, respectively. The system allows to test 1–4 injectors at the same time. In this study, only one injector is tested, and three holes connecting the pipes with a measuring chamber are simply blocked. The high-pressure pump is a DENSO model (HP3) driven by a DC motor. The rail is a practical rail in a four-cylinder common rail engine and includes a pressure transducer located in one end and a controlling pressure control valve (PCV) located in the other end. The high-pressure pump is equipped with a suction control valve (SCV). The management system will use the rail pressure signal to control the PCV and SCV so that the rail pressure can be managed according to each operating condition. This is similar to the practical system in common rail engines.

To measure the pipe pressure, a Kistler 4067A3000 piezoelectric transducer is located in the pipe before the injector. The injector is operated directly into an IR measuring chamber. In this chamber, a high-response Kistler transducer (4075A100) and its amplifier are used to monitor the chamber pressure. The chamber is fully filled with diesel, which is the fuel tested in this study and initially compressed at 40 bars. This pressure is relevant to the pressure condition at the time of injection in practical common rail engines. After each injection, the additional amount of fuel forced by the injector in the measuring chamber is released using a fast-response release valve so that the pressure in the chamber will quickly be readjusted back to 40 bar as an initial condition. The pressure variation in the chamber during the injection process is used to compute the IR. The released fuel amount is measured by a mass flow meter (Coriolis-type, Siemens Mass Flow 2100) so that the total amount of fuel injected is quantified. Energizing pulse is applied to the injector through the management system, and this signal will be recorded using a current probe TA-189. This system is controlled by a self-developed software established in LabVIEW environment. More details about this system can be found in Ref. [20].

High-pressure pipes are used to connect the common rail and injectors. In this study, the high-pressure pipes are simply called pipes. This study examines only one injector although the system allows testing up to four injectors at the same time as previously mentioned. During the injection, both rail pressure and pipe pressure are variable. However, variations in the pipe are much bigger and easier to notice due to the pipes' much smaller size compared to that of the rail and shorter delay time from the injector nozzle. Thanks to the noticeable variations in the pipe pressure during the injection, the pipe pressure signal could be more directly represent the hydraulic behaviors related to the injection events. In this work, two pressure transducers are used to measure both pressure in the common rail and pressure in the pipe. One transducer is located at one end of the common rail, while the other is located in the pipe, just before the injector. The rail pressure variations are also due to the high-pressure pump and PCV. Combinations of these two pressure signals could be useful in describing the hydraulic behaviors in the system. In this study, p_{rail}, also known as injection pressure, is the nominal pressure in the common rail. $p_{railpipe}$ is the actual pressure in the common rail and measured using transducer #2 shown in Fig. 1 p_{pipe} is the pressure in the high-pressure line and measured by pressure transducer #3 shown in Fig. 1. The nominal pressure, p_{rail}, is the pressure controlled by the ECU, and this nominal value is constant for each operating condition. The actual pressure in the common rail, $p_{railpipe}$, is variable, and this is due to the injection events and the pressure fluctuations/oscillations in the common rail.

Fig. 2 shows a cross-sectional view, including important dimensions such as the length and diameter of the pipeline and the dead volume, of the CRI2.2 injector tested in this study. The figure also shows the location of transducer #3 measuring the pipe pressure, p_{pipe}. The flowing distances from the transducer #3 to the controlling chamber and the injector nozzle are 170 and 330 mm, respectively. The flowing distance from the transducer to the common rail (not shown in this figure) is 420 mm [18]. Assuming 1500 m/s as reference speed of sound considering the transducers' positions [3], the wave transmission times from the nozzle and the controlling chamber to the pipe pressure transducer #3 are 0.22 ms and 0.113 ms, respectively. Similarly, the wave transmission times from the nozzle and the controlling chamber to the common rail pressure transducer #2 are 0.41 and 0.51 ms, respectively.

3. Investigating conditions

In this study, hydraulic behaviors of a second-generation common rail solenoid injector introduced in Section 2 operating under single and split injection modes will be investigated. Here, split injection is limited to double shot injection, and the single modes are called solo injection. Events that happen in the first and second shots and the influence of the first shot to the next will be explored. In the solo injection mode, a wide range of energizing time (ET) from 0.3 to 2.0 ms is investigated; therefore, the injector is partly or fully opened. A wide range of rail pressure from 600 to 1400 bar is also tested. Fig. 3 shows the testing points used for the split injection mode investigated in this work. The rail pressure tested in double injection mode is equivalent to the solo mode, and the DT varies between 0.2 and 2 ms, as shown in Fig. 3. For the split injection mode, three nominal injection ratios (30/70, 50/50, and 70/30 by volume, respectively) between two shots are investigated.

To operate the system under split injection modes, it is critically important to determine the actual injection rates for the first and second shots. The actual rates are affected by ETs and injection ratios and the influence pressure oscillation created by the first shot on the second shot. Firstly, correlations between the total fuel injection volume and ET in the solo injection mode are developed. Based on these data, the first and the second energizing time (ET_1 and ET_2, respectively) of the double shot mode will be estimated according to the nominal volume ratios of 30/70, 50/50, or 70/30. The estimations are done without accounting for the influence of the first shot on the second shot, and this explains why the ratios are called "nominal". The hydraulic characteristics (e.g., differences between volume measured and the nominal amount, the trends in pressure drop and pressure recovered in the fuel rail) observed from the tests indicate the influence of the first shot on the second shot in the split injection strategy.

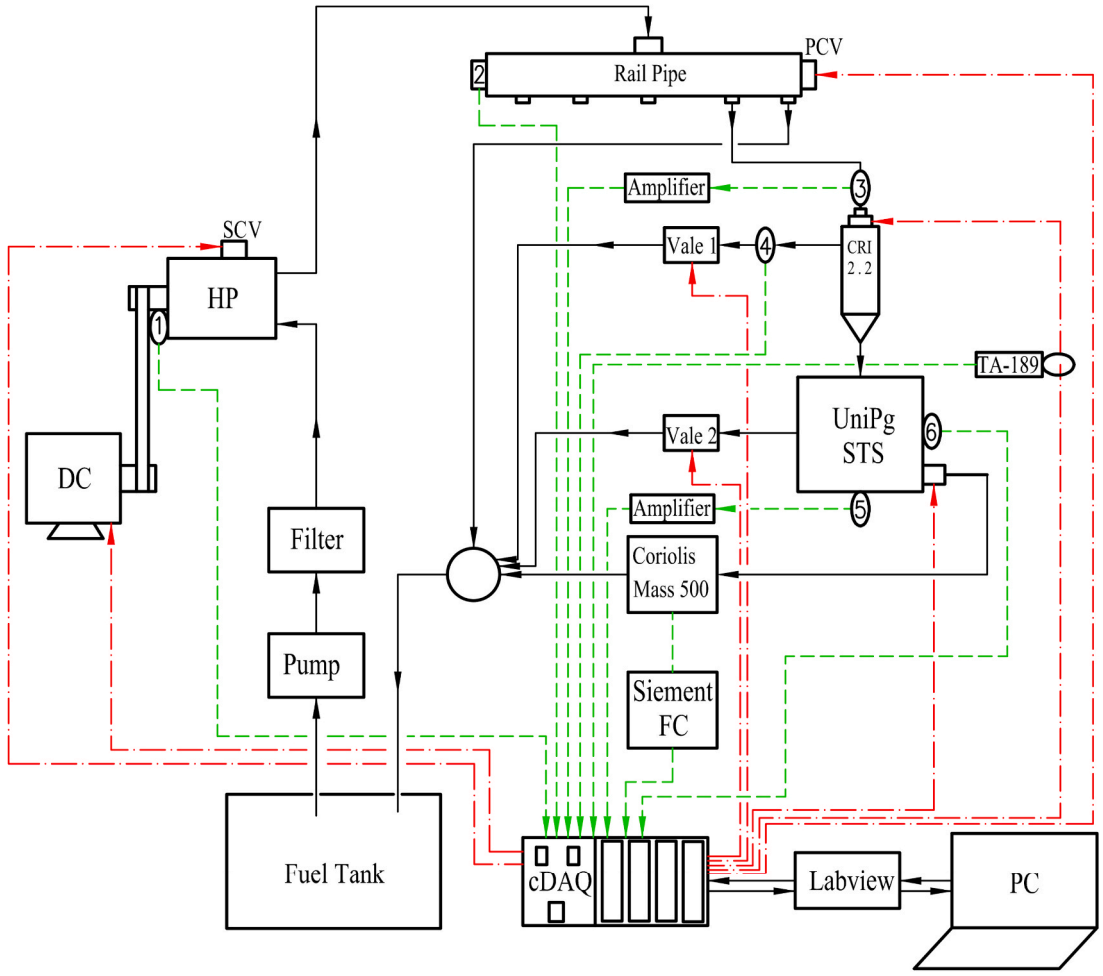

DC, DC motor; HP, high-pressure pump; UniPg STS, Injection Analyzer Shot-to-Shot; SCV, suction control valve; PCV, pressure control valve; Valve 1, fast-acting solenoid valve controlling the back leak pressure; Valve 2, safety valve; 1, encoder; 2, fuel common rail pressure sensor; 3, fuel pipe pressure sensor; 4, fuel back leak pipe pressure sensor; 5, fuel pressure sensor in the measuring chamber; 6, fuel temperature sensor in the measuring chamber; TA189, ampere.

Fig. 1. Experimental setup.

4. Results and discussion

4.1. Solo injection

To improve the measuring uncertainty and to eliminate the random characteristic, studying the injection process requires a number of consecutive injections. In this study, 400 consecutive injections will be recorded. The first 100 injections need to stabilize the hydraulic system, while the following 300 consecutive injections are recorded to examine the hydraulic characteristics. This is applied for both single and split injection modes.

It is critically important to note that two types of instabilities exist in the injection systems: (i) inter-cycle instability due to the random nature characteristics and (ii) deviations in the course of subsequent injections from the ideal conditions for a single injection, which are systematic. These types of instabilities are difficult to be exactly separated because they simultaneously occur. It is also very challenging to set up ideal conditions for an injection mode to examine the injection deviations due to the randomness of injection process. In this work, the inter-cycle instability has been evaluated using the COV, while the deviations are examined through SD of IRs. The COV values of pressure, injection rate, and energizing pulse of 300 shots have been investigated. The COV values of those parameters are computed similarly to the COV of IMEP reported in Ref. [21]. Another approach that is normally adopted in the literature to quantify system uncertainty is to use the sum of square roots of uncertainties of main items in the experiment system. Although this is not quantified here, the SDs of fuel volume through 300 shots also include the system characteristics.

Fig. 4a shows an example of IR signals recorded in 300 consecutive injections as mentioned above, and this is for a solo injection mode under p_{rail} = 1000 bar and ET = 1 ms. It is clearly shown that the maximum difference in the injection process is observed when the IR is highest during the injection process, which is approximately 2 mm^3/ms (see the enlarged window shown in Fig. 4a). As shown in Fig. 4, at the end of the fuel injection process, IR suddenly downs to zero (about 2 ms after the ET starts) and then fluctuates around this value. This

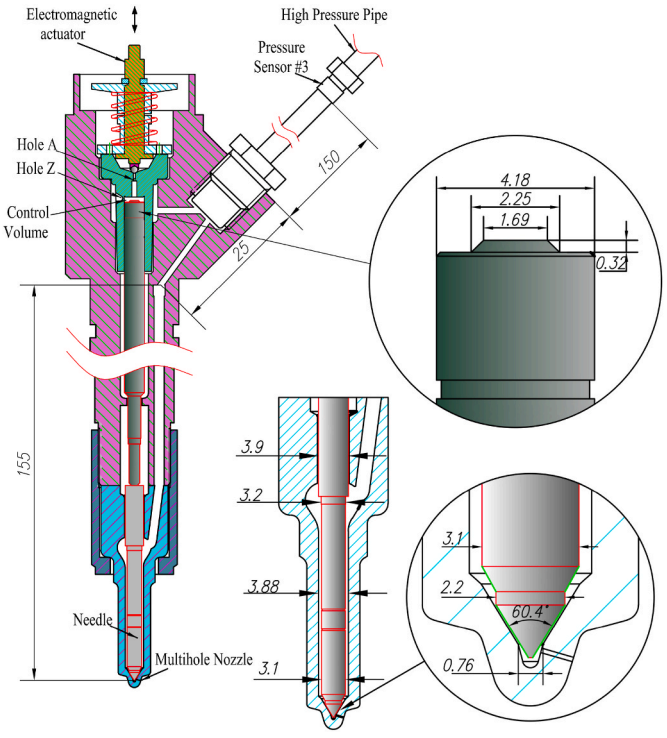

Fig. 2. Schematic sketch of the CRI2.2 injector.

fluctuation is due to the pressure oscillations in the measuring chamber. This is in agreement with Postrioti et al.'s work [20]. This example shows a confidence to use averaged values from 300 consecutive cycles to analyze the hydraulic characteristics of the injector, and the averaged values will be used throughout this work.

Fig. 4b shows the SD of injection rates of 300 shots under single injection strategy. It shows that the deviation among those 300 shots is quite small. Under p_{rail} = 1000 bar and ET = 1 ms, SD of the injection rates is 0.087 mm^3/shot, which corresponds to 0.13%. Fig. 4c shows COV values of injection rates under various rail pressure and ET conditions. It is clear that the rail pressure has a minimal effect on the COV, while the influence of ET on the inter-cycle variation is significant. Longer ET leads to better stability. This is expected as the periods of needle lifting, maintaining, and closing are longer to stabilize the injection process. It is interesting to note that the COV of injection rates observed here corresponds with the COV of IMEP of diesel engines under table operating conditions. The COV of injection rates shown in Fig. 4c are between 0.5% and 2%. Heywood [21] reported that the stability limit for compression ignition engines is reached when the COV of IMEP value exceeds 2%. This implies that the inter-cycle variation of the injection system might be the main contribution to the diesel engine cycle-to-cycle variations.

Fig. 5 shows four different signals (energizing pulse, IR, p_{pipe}, and $p_{railpipe}$, respectively) representing hydraulic characteristics observed for solo injection modes under p_{rail} = 1000 bar and ET = 1 ms. From Fig. 5, special events, including start of energizing (SOE), SON, SOI, and EOI, are isolated using those signals. These events were introduced earlier in Refs. [2,20,22–25]. Further investigations will be provided here. Special events, including SOE, SON, SOI, and EOI, are noted in the IR curve in Fig. 5 as the points indicated by numbers inside circles, ①, ②, ③ and ④, respectively. Point ① (SOE, t = 0 ms) is identified as the start of the driving current profile from the current probe. Point ②, SON, is characterized as the point where IR becomes negative after SOE. Point ③, SOI, corresponds with the time IR that becomes zero again from point ②. When the nozzle opens (SON), it acts as a piston. When the nozzle moves up rapidly, a small volume of fuel is quickly "pumped" back to the injector, which leads to the pressure drop in the measuring chamber, resulting in negative IR as mentioned above. It is noted that the negative IR behavior was previously reported in some references related to Bosch and Zeuch measuring approaches [20,26–29]. The fuel from the high-pressure rail quickly stops the drop and SOI ③ occurs when the IR is positive as noted above. The duration showing negative IR is only about 0.13 ms as observed in this study. IR increases quickly, reaches maximum value for a while, and then drops quickly when the nozzle closes. Point ④, EOI, is noted when IR becomes zero again on the right side, as shown in Fig. 5. After point ④, IR is fluctuating, as mentioned above.

In the pipe and rail pressure signals, SOE could be noted as points ① and ①', respectively. Points ① and ①' are characterized by small peaks in those signals, as shown in Fig. 5. This could be attributable to the pilot stage opening. Here, it is noted that the time shown in Fig. 5 is a reference for energizing, where ET starts from 0 ms. In the starting event, the electromagnetic disturbance created by the V_{boost} may initiate the ball in hole A (see Fig. 2), which may lead to the spikes observed in p_{rail} and p_{pipe} corresponding to points ① and ①', respectively. However, these spikes are quite small and require further investigation. SOI is also quite easily noted in rail and pipe pressure signals where the pressure is suddenly dropped, and an observable change is observed in the slope noted as points ③ and 3" indicated in Fig. 5. Delay times between events isolated using current pulse, pipe, and rail pressure (e.g., ①, ①, and ①') are due to hydraulic, electronic, and mechanical delays [2,20,30].

SOI leads to significant drops in both rail and pipe pressure; however, pressure drop is observed prior to SOI. When electric pulse is applied to the injector, it acts for the solenoid valve to open hole A. This leads to pressure reduction in the controlling chamber and as such pressure drops in both pipe and rail prior to SOI. At this point, although hole A has been opened, pressure in the controlling chamber is still high enough

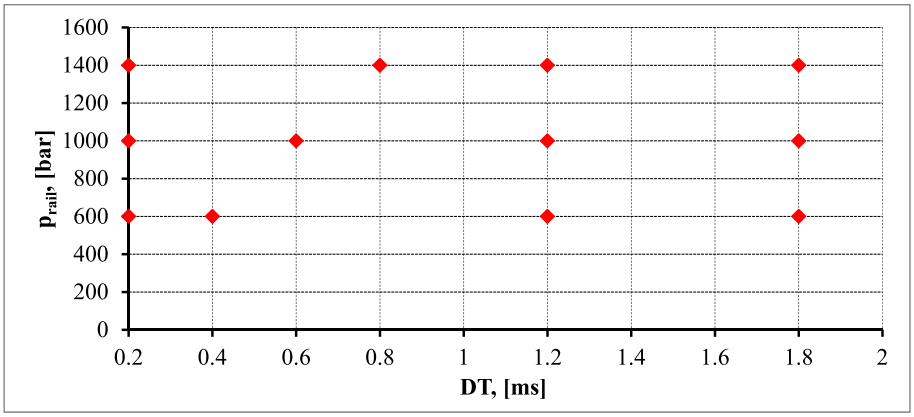

Fig. 3. Testing points used for the split injection modes.

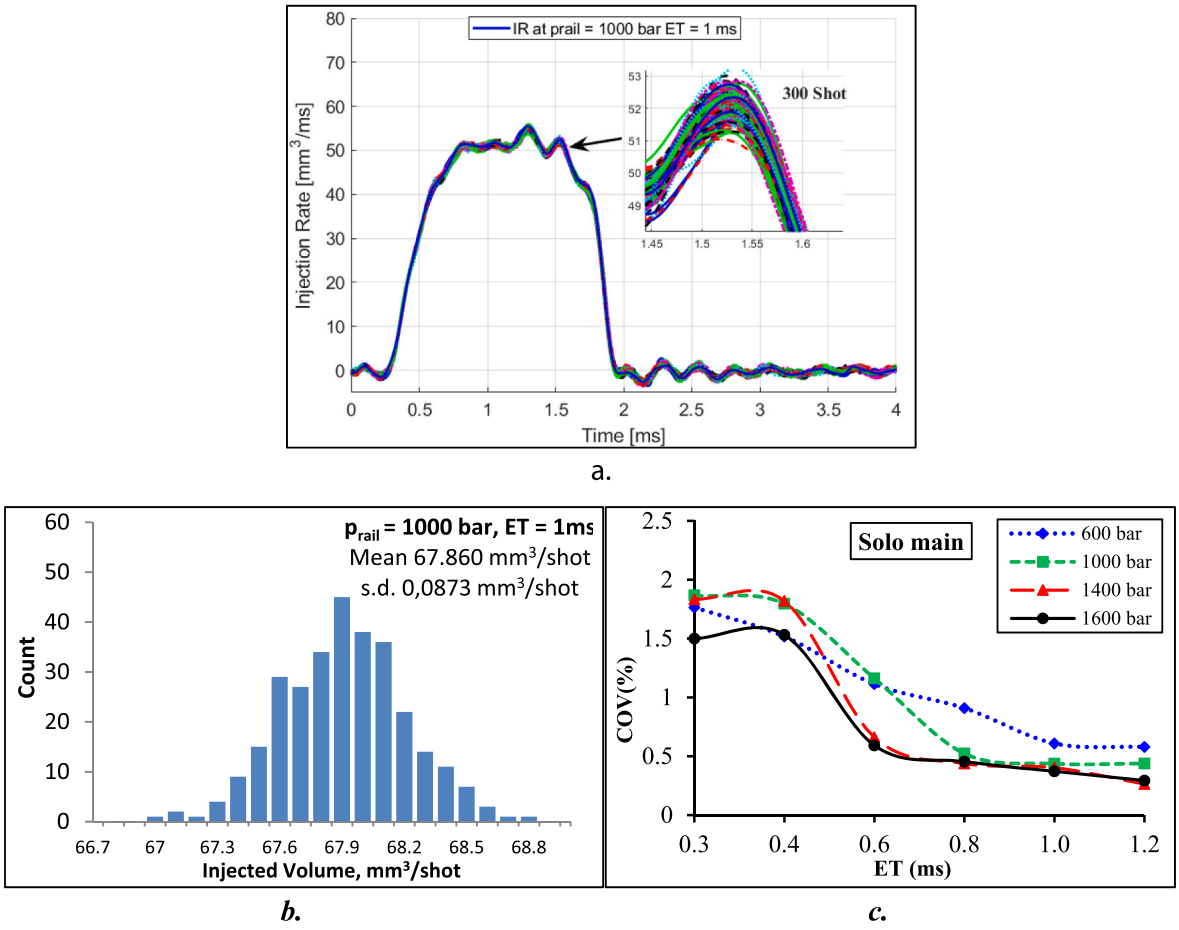

Fig. 4. a. Example of injection rates of 300 consecutive injections; b. standard deviations of injection rates of single injection mode under solo injection mode with p_{rail} = 1000 bar and ET = 1 ms; c. Coefficient of variation (COV) of injection rates under different ET times and rail pressure.

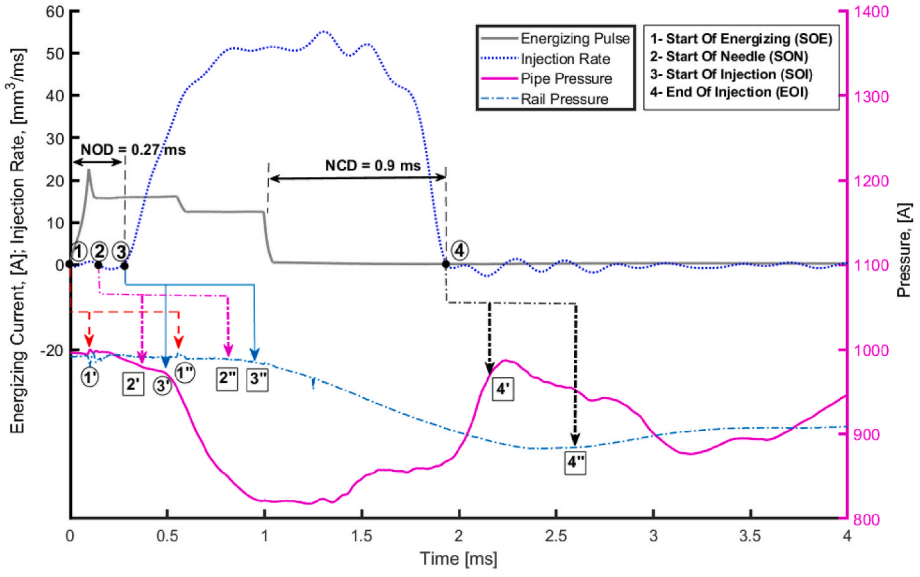

Fig. 5. IR, $p_{railpipe}$, and p_{pipe} under p_{rail} = 1000 bar, and ET = 1 ms

to prevent the nozzle to be lifted up. Therefore, a slight reduction of the rail pressure is observed although injection at this point has not started yet.

Delays due to pressure wave transmission in the pipe and rail can be observed in Fig. 5. It is important to note that the points indicated by numbers inside circles (e.g., ①, ②, ③, ④, and so on) can be easily determined. However, the points located inside the square are estimated using their corresponding points that can easily be determined. The arrows shown in Fig. 5 imply this approach (e.g., points 4′ and 4″ can be located using ④). From SOI, the pressure wave transmission from the

injector to the pipe pressure transducer (item #3 as shown in Fig. 1) is about 0.22 ms, and that to the rail transducer (#2 as shown in Fig. 1) is 0.51 ms approximately. Using these delay times, EOI could be noted in the pipe and rail pressure signals (see points 4' and 4"). It is clear that points 4' and 4" are quite difficult to be exactly isolated although point 4' is quite close to the location where the pipe pressure reaches maximum.

By investigating the p_{pipe} curves under three energizing conditions (ET = 0.3 ms, 1.0 ms, and 1.2 ms, respectively), Fig. 6 shows the influence of energizing time on the hydraulic characteristics of the pipe pressure signals. It is shown that ET does not affect the first periods of the injection process (see points ① to ③). The delay from ① to ③ is around 0.27 ms with a pressure reduction of about 2–3% from the pipe pressure at point ① regardless of the ET conditions tested here. A small difference between those signals in the first periods for different ET conditions is attributable to the oscillations of the pipe pressure created by RPCV and PCV. These valves work to maintain the rail pressure under different circumstances. Thanks to these valves, the pressure in the rail and therefore in the pipe is oscillating.

It is also shown that increasing ET leads to a bigger pipe pressure reduction ($p_{pipeRed}$). However, up to a certain ET when the needle reaches its maximum stroke, the reduction remains the same (e.g., it fluctuates around 180–190 bar as shown in Fig. 6 when operating under ET = 1 ms and 1.2 ms). Fig. 7 now plots the pressure drop determined by the injection event, here called $p_{pipeRed}$, observed for ET = 1 ms and different p_{rail} conditions (from 600 to 1600 bar). It is clear that the higher rail pressure, the bigger the pressure reduction, $p_{pipeRed}$, because the same ET at higher p_{rail} determines larger injected quantity and thus bigger pressure drop.

Another phenomenon that can be observed in Fig. 7 is the under-recovering pressure. After the pressure reduction, in the nozzle closing up stroke, the pipe pressure is recovered and reaches a value that is lower than the nominal common rail pressure, p_{rail}. The difference between the maximum value and p_{rail} is now called p_{under}, which is equal to the maximum value of p_{rail} (at the EOI) minus the nominal pressure. In some cases at low p_{rail} (e.g., p_{rail} = 600 bar, as noted in Fig. 7), the rail pressure could be more than recovered, and as such, p_{under} is positive. This will be further explored later in Fig. 8b. As generally seen from Fig. 7, higher p_{rail} leads to bigger p_{under}. This is understandable as a smaller reduction helps to recover the pressure easier.

Fig. 8 shows $p_{pipeRed}$ (Fig. 8a) and p_{under} (Fig. 8b) as a function of p_{rail}. As clearly shown in Fig. 8a, increasing ET increases $p_{pipeRed}$. Fig. 8a also shows that higher p_{rail} leads to bigger $p_{pipeRed}$. Here, it is noted that $p_{pipeRed}$ is almost linear with p_{rail}. It is interesting for the whole rail pressure range investigated here that the reductions observed for these pressure conditions are approximately 20% of p_{rail}. Fig. 8b shows that increasing ET generally leads to a reduction in p_{under}. Generally, p_{rail} has some influences on the recovering process; however, these influences are quite difficult to quantify since there exist different hydraulic processes simultaneously occurring in the injection process, such as working process of PRCV and PCV as mentioned earlier. Fig. 8b also shows that under low p_{rail} and/or short ET, the rail pressure could be over-recovered, the maximum rail pressure at the end of recovering process is bigger than the nominal pressure, and p_{under} is positive as briefly mentioned above. Moreover, when ET is shorter than 0.6 ms, p_{under} is positive. This is also true when ET = 0.8 ms with p_{rail} = 1000 bar or lower.

4.2. Split injection

To investigate the hydraulic characteristics when the injector is operating under split injection mode, Fig. 9 shows an example of current pulse, IR, and p_{pipe} signals under p_{rail} = 1000 bar, DT = 1200 ms (duration from the end of the first energizing pulse to the start of the second energizing pulse), and $ET_1 = ET_2 = 0.6$ ms. Here, it is noted that a solo injection mode was investigated under ET = 0.6 ms earlier, and this is a good database to compare the first shot of the double shot mode investigated in this section. In this study, it is observed that the IR and p_{pipe} signals obtained from the first shot of the split injection mode are almost identical with the single injection mode with ET = 0.6 ms described earlier.

Similarly to the special events described for single injection mode presented earlier, the events that happen in the split injection mode are double compared to those in the single shot modes. Events such as SOE (①), SOI (②), and EOI (③) of the first shot are described here similarly to that in the single shot modes. The corresponding events that happen in the second shot will be described here as Roman numerals Ⅰ, Ⅲ, and Ⅳ for SOE, SOI, and EOI, respectively, as shown in Fig. 9. Those special events are also described in the pipe pressure curve. In this curve, points ① and ③ can be isolated directly using the peak in the beginning period and the change in the slope as discussed earlier in the single injection mode. Other events are determined using the time period obtained in the IR curve.

Fig. 9 shows significant differences in both IR and pipe pressure

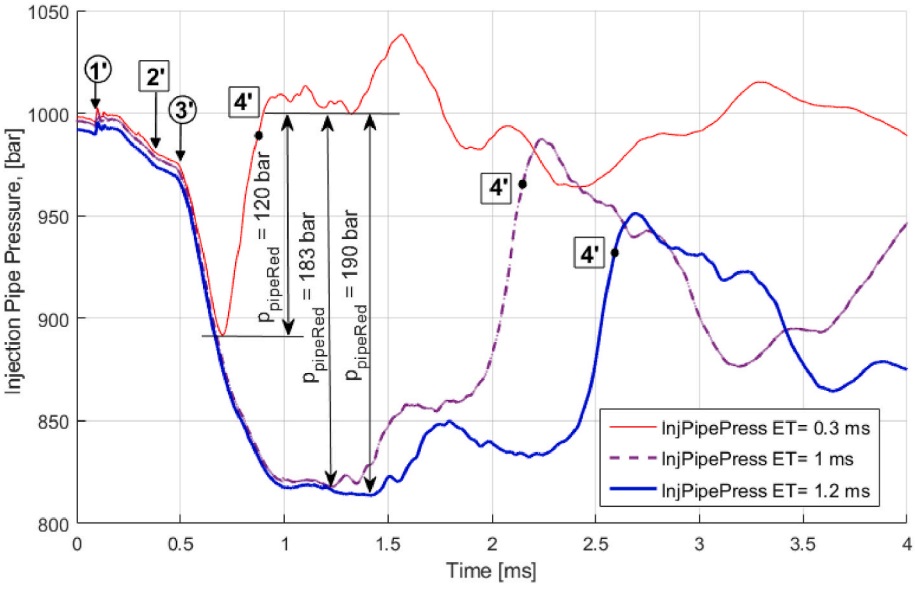

Fig. 6. p_{pipe} of solo injection modes under p_{rail} = 1000 bar, three ET conditions (0.3, 1.0, and 1.2 ms, respectively).

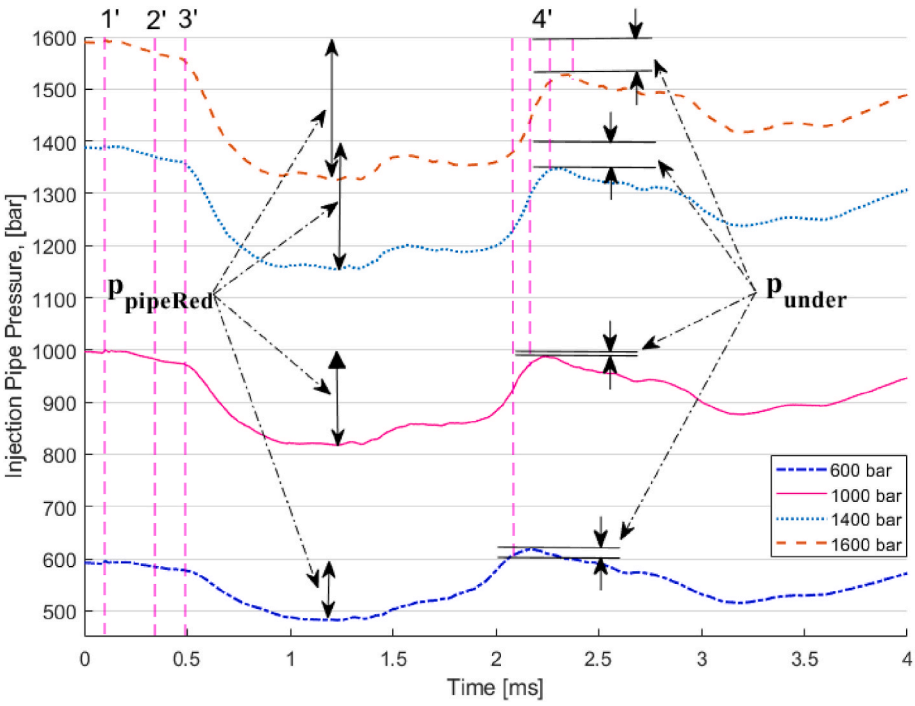

Fig. 7. *$p_{pipeRed}$ and p_{under} of single injection modes under ET = 1 ms and p_{rail} varying from 600 to 1600 bar.*

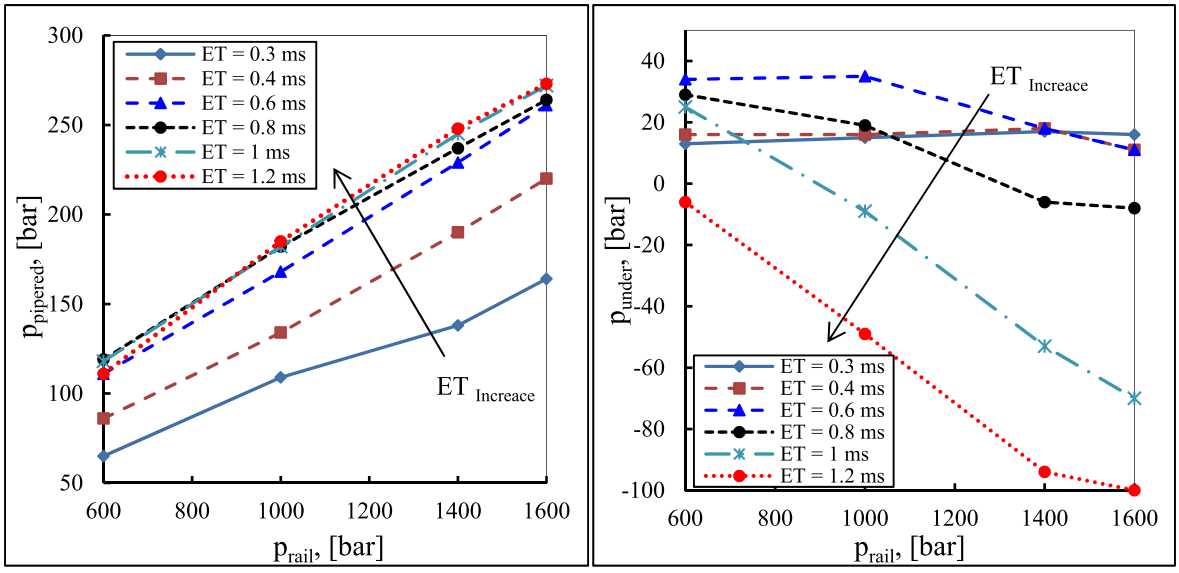

Fig. 8. (a) Pipe pressure reduction, $p_{pipeRed}$; (b) Under-recovering pipe pressure, p_{under} versus p_{rail}.

observed for the two shots, although ET_1 and ET_2 investigated here are similar. As $ET_1 = ET_2$, the differences indicate the influence of the first shot on the second one in this split injection mode. The influence is mainly due to the pressure wave oscillation in the first shot (as mentioned in the single injection mode). The influence on IR and p_{pipe} of the first and second shots in the split injection mode is clearly observed in Fig. 9. This influence varies with DT, the injection ratio between these two shots, and rail pressure. This is investigated in the following sections.

To investigate the influence of DT on IR and p_{pipe}, Fig. 10 shows IR and p_{pipe} curves under $p_{rail} = 1000$ bar, $ET_1 = ET_2 = 0.6$ ms, and DT varying from 0.2 to 1.8 ms. For comparison purposes, IR and p_{pipe} of the solo injection mode under ET = 0.6 ms are also provided. Information of the solo injection mode is also helpful to investigate the influence of the first shot to the second one in the split injection mode. As shown in Fig. 10, IR and pressure curves of the first shot are almost identical to those of the solo injection mode. Qualitatively, as can be seen from Fig. 10, the maximum IR and minimum p_{pipe} of the second shot significantly vary with DT (see arrows shown in Fig. 10). It shows that DT and the pipe pressure oscillation after the first shot have significant effects on IR of the second shot. The trend of maximum IR during the second shot (see arrows at the top of IR curves during the second shot) is also

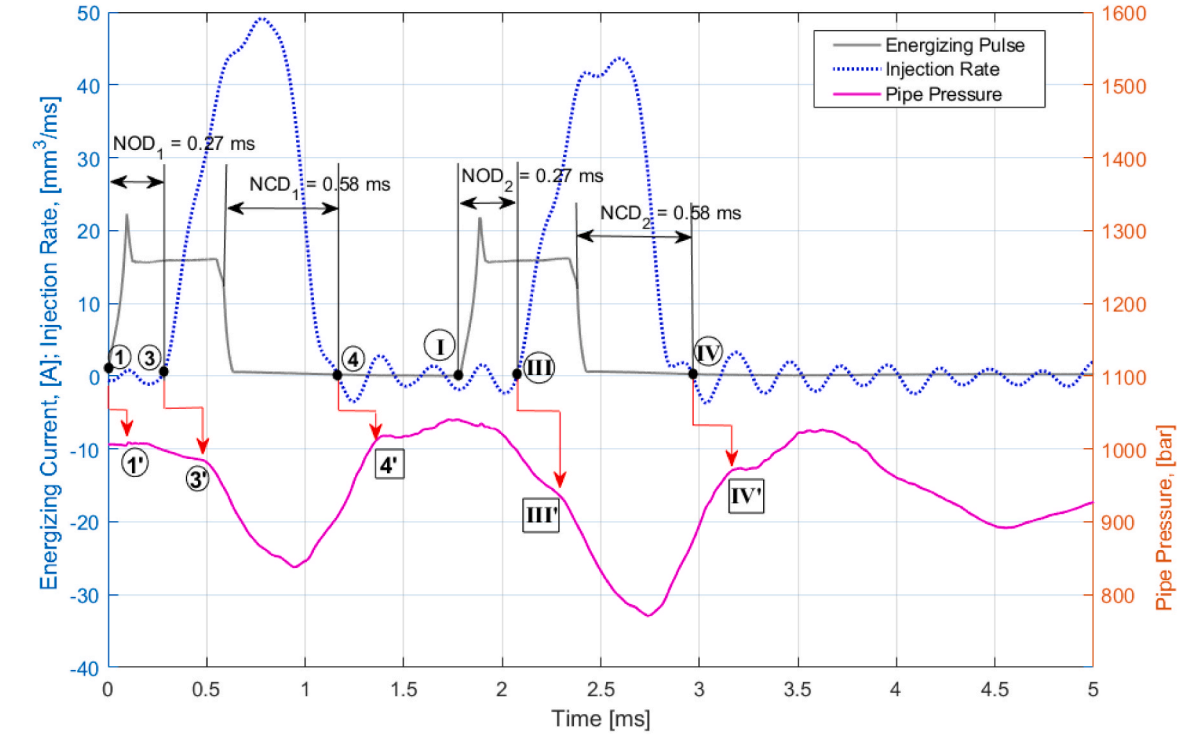

a.

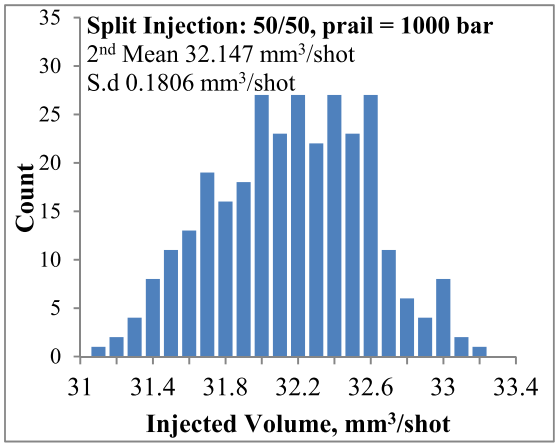

b.

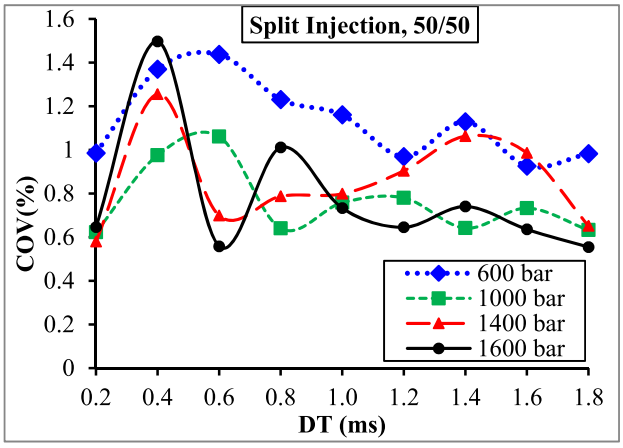

c.

Fig. 9. a. IR and p_{pipe} of split injection modes under p_{rail} = 1000 bar, $ET_1 = ET_2$ = 0.6 ms, DT = 1200 ms; b. standard deviations of injection rates of split injection mode (50/50, p_{rail} = 1000 bar, DT = 1200 ms); c. coefficient of variation (COV) of injection rates of split injection mode (injection ratio: 50/50) under various DT and rail pressure.

identical to the trend of the minimum pipe pressure during the second shot (see two arrows at the bottom of the pipe pressure curves during the second shot).

Fig. 10 also shows the start of injection of the second shot, SOI_2 (see the small black circles in p_{pipe} curves in Fig. 10). It is interesting that SOI_2 pointing under different DT is almost following the trend of pressure curve of the solo injection mode with ET = 0.6 ms (see the dashed black curve with the red indicated arrow).

Similar investigations for standard deviation and COV of IRs for single injection modes reported in Fig. 4, SD and COV of IRs are shown in Fig. 9b and c, respectively, for split injection modes. Fig. 9b shows an example of SD of the second shot for injection ratio of 50/50, p_{rail} = 1000 bar, and DT = 1200 ms. It gives an SD of 0.1806 mm^3/shot, which corresponds to 0.6%. Fig. 9c shows COV of IRs of split injection modes under various rail pressure and DT conditions. It shows that COV fluctuates between 0.6% and 1.6%, which is also identical with the COV of IMEP of diesel engines as discussed earlier. DT has a slight effect on COV, that is, longer DT leads to smaller COV, as shown in Fig. 9c.

From the literature, it is noted that for multi-injection modes having a solo-main injection, pilot injection has a little effect on the main injection, while the main injection significantly affects the post injections. However, this current work aims to investigate split injection, where the main injection is divided into two shots under small DT as mentioned earlier. In the split injection modes, the first shot may be in the position of the pilot injection in multi-injection modes, while the second shot may correspond to the post injection in multi-injection strategies.

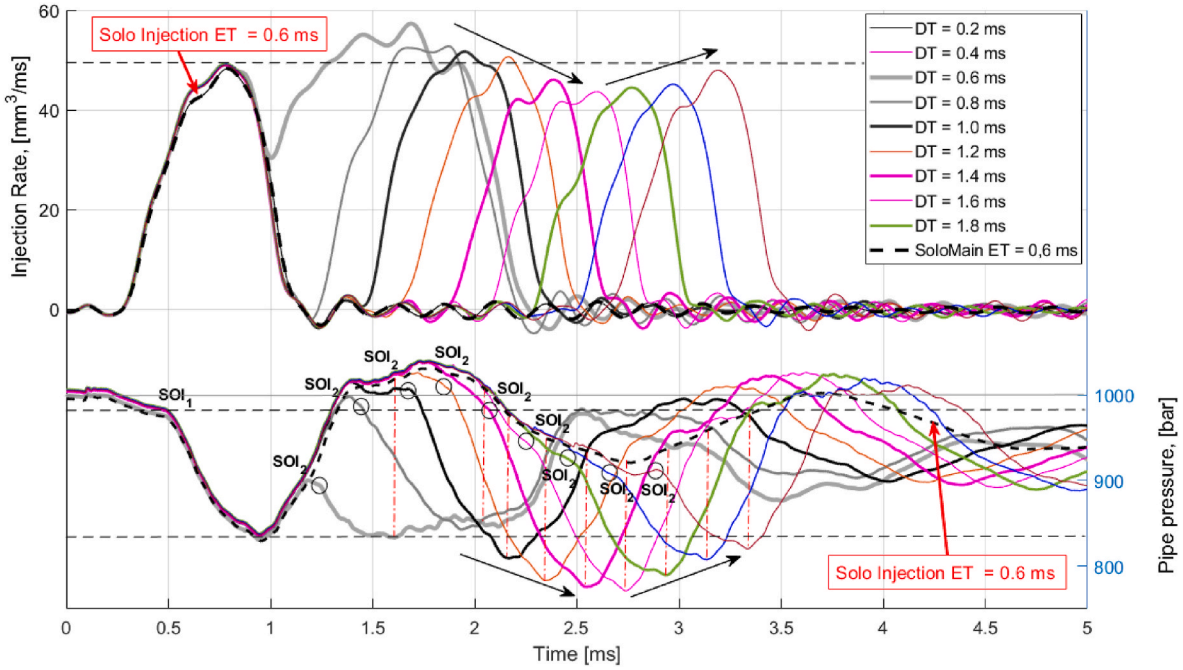

Fig. 10. IR and p_{pipe} under $ET_1 = ET_2 = 0.6$ ms, $p_{rail} = 1000$ bar and varying DT.

However, in the split injection, the amount of fuel injected in each event is much bigger than a typical pilot or post event. Furthermore, in the split injection mode, DT is much shorter, so the influence of the first shot to the second could be more significant. The influence of the first shot to the second one in two cases, injection ratios 30/70 and 70/30, respectively, is now investigated, as this may show similar issues with the influence of pilot injection to the main and the main to the post.

Fig. 11a and b shows the IR curves of split injection under injection ratios of 30/70 (Fig. 11a) and 70/30 (Fig. 11b) and various DT. It generally shows that DT has significant effects on the IR, that is, longer DT leads to smaller effects. In the case of injection ratio of 70/30 (Fig. 11b), the influence of the first shot to the second one is more significant. This is in good agreement with the influence of the main injection on the post injection in multi-injection modes. Variations in the IRs of the second shot under the injection ratio of 30/70 is about 6 mm^3/ms (approximately 10.3%), while this value is 16 mm^3/ms

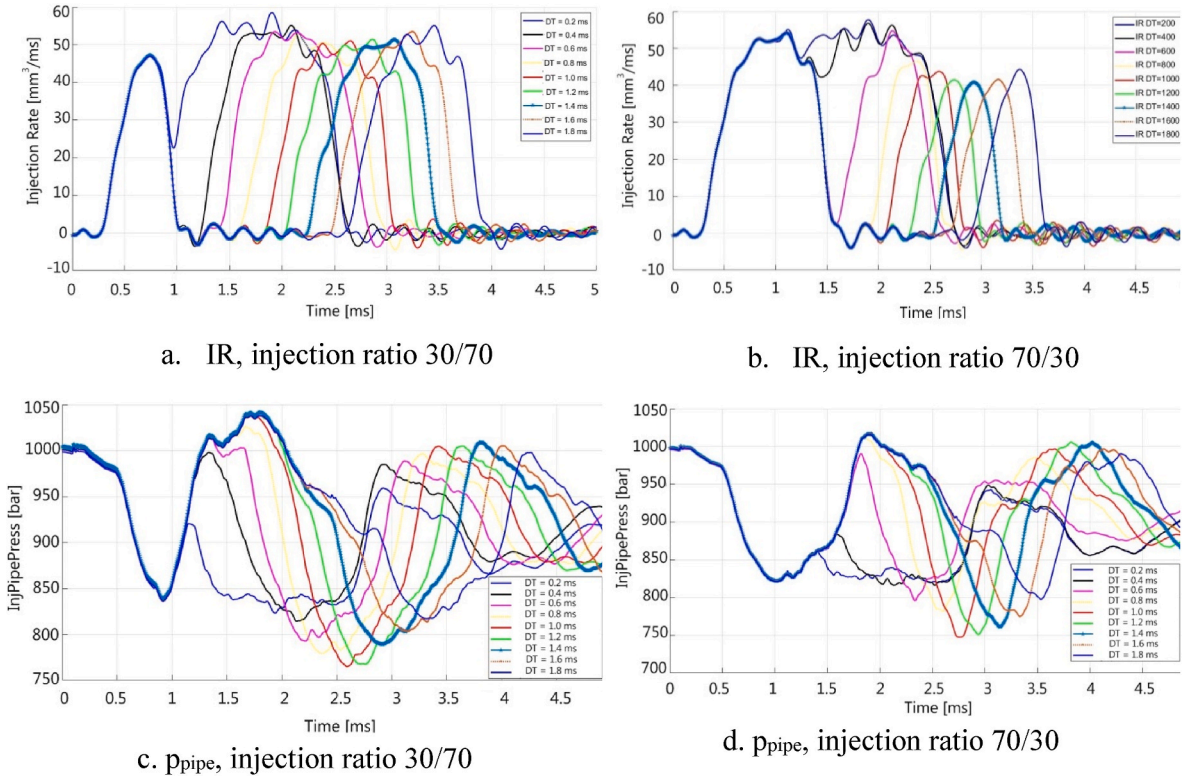

Fig. 11. IR (11a and 11b) and p_{pipe} (11c and 11d) of split injection modes under $p_{rail} = 1000$ bar, injection ratio of 30/70 (11a and 11c) and 70/30 (11b and 11d).

(approximately 28%) under the injection ratio of 70/30.

Fig. 11c and d shows p_{pipe} curves of split injection under the injection ratios of 30/70 (Fig. 11c) and 70/30 (Fig. 11d) and various DT. It shows that the pressure drop of the first shot under the injection ratio of 30/70 (Fig. 11c) is around 160 bar and smaller than that under the injection ratio of 70/30 (175 bar as shown in Fig. 11d). The smaller pressure drop leads to faster rail pressure recovering time, resulting in higher rail pressure at the beginning of the second shot, as shown in Fig. 11c and d. The higher recovering pressure also leads to bigger oscillation in the pipe, resulting in bigger fluctuation in the injection rate. This is evident by closely observing the injection rate curves shown in Fig. 11a and b. The injection rate curves during the second shot shown in Fig. 11a for the injection ratio of 30/70 show more local peaks with respect to that shown in Fig. 11b for the injection rate of 70/30.

The trend of minimum p_{pipe} of the second shot is also noted here. To examine the trend, let's draw vertical lines (see dashed red lines) from the location of minimum p_{pipe} of the second shot and to the pressure curve of the solo injection mode provided here (dashed black curve). The lengths of vertical lines are called different pressure and plotted versus DT in Fig. 12 for further investigation.

The different pressure shown in Fig. 12 could help to examine the impact of rail pressure on the different pressure. As clearly shown from Fig. 12, DT has a small impact on the different pressure. The difference mainly depends on p_{rail}, that is, higher p_{rail} leads to bigger different pressure. This indicates that the variations in p_{pipe} and IR curves of the second shot mainly depend on the oscillations of pipe pressure that is created at the end of the first shot.

Fig. 13 shows IR and p_{pipe} curves of split injection modes under $ET_1 = ET_2 = 0.56$ ms, and DT = 1 ms and three different rail pressure conditions (1000, 1400, and 1600 bar, respectively). Under the operating conditions investigated here, the profiles of IR and p_{pipe} of the two shots are quite similar. However, closely examining the start and end of the second shot shows that deceasing p_{rail} slightly advances the SOI of the second shot while slightly retards the EOI of the second shot (see enlarged windows in Fig. 13). Differences also exist between minimum pressure values of the first and the second shots (48, 64, and 70 bar corresponding to 1000, 1400, and 1600 bar of p_{rail}, respectively). These differences are around 5% of the rail pressure. The lower minimum pressure of the second shot compared to that of the first shot is attributable to the pressure oscillation created by the first shot.

As shown in Fig. 13, under the rail pressure condition of 1600 bar, the pipe pressure curves qualitatively show their lower smoothness level compared to those observed under other pressure conditions. This is quite clear at the ending periods of the first and second shots (e.g., around 1.5 ms for the first shot and 2.75 ms for the second shot as shown in Fig. 13). The rail pressure condition of 1600 bar lies in the highest pressure range of common rail injection systems, and the high-pressure condition may lead to higher level of pipe pressure oscillation. It was also mentioned earlier that higher rail pressure results in higher difference between minimum pressure of the first and second shots, as shown in Fig. 11 and bigger p_{under} as shown in Fig. 7.

Due to the shot-to-shot variation of the IR in the split injection mode as discussed above, the total volume injected in the second shot varies according to parameters driven by the split injection mode, especially DT. It is critically important to quantify the total volume injected for both shots to ensure the right amount of fuel supplied to the engine under these injection modes. Fig. 14 shows the total fuel volumes injected in two shots, V_1 and V_2, respectively, under a wide range of DT from 0.2 to 1.8 ms and three different injection ratios (30/70, 50/50, and 70/30, respectively).

Fig. 14 also provides nominal lines or calculation values for the injection volume. These nominal values are calculated to determine ET_1 and ET_2 for three different injection ratios (30/70, 50/50, and 70/30, respectively) investigated in this study. As shown in Fig. 14, the total fuel volume injected by the first shot is quite stable and follows the nominal lines while that injected by the second shot fluctuates with DT. Under DT < 0.8 ms, the difference between V_2 and the nominal value is significant. A short DT leads to significant fluctuations in the pipe pressure, especially in the case where an overlap exists between two shots. V_2 is normally higher than the nominal values, and this is true for all cases investigated here. When DT exceeds 0.8 ms, the shot-to-shot influence is impaired, and V_2 is closer to the nominal lines. Practically, this issue needs to be addressed to control the injector supplying the right amount of fuel as expected.

5. Conclusion

In this study, hydraulic characteristics, including inter-cycle instability of a second-generation solenoid common rail injector operating under solo injection and split injection strategies, have been investigated successfully. Different from solo injection, in the split injection mode, the influence of the first shot on the second shot is significant, affecting the actual fuel IR and fuel volume injected by the second shot. Important outcomes obtained from this study can be summarized as follows:

1. Two types of instabilities exist in the injection systems: (i) inter-cycle instability due to the random nature characteristics and (ii) deviations in the course of subsequent injections from the ideal

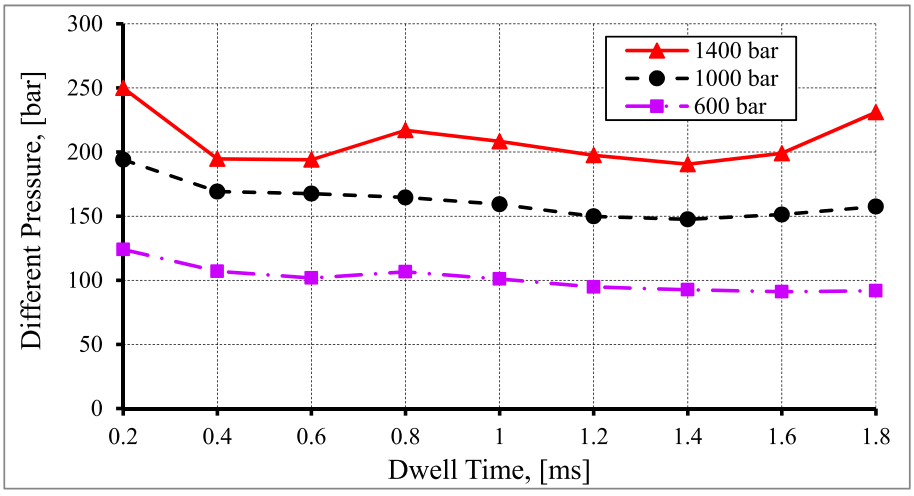

Fig. 12. Different pressure (vertical lines from minimum p_{pipe} of the second shot and to the pressure curve of the single injection mode, introduced in Fig. 10) versus DT, under three p_{rail} conditions (600, 1000, and 1400 bar, respectively).

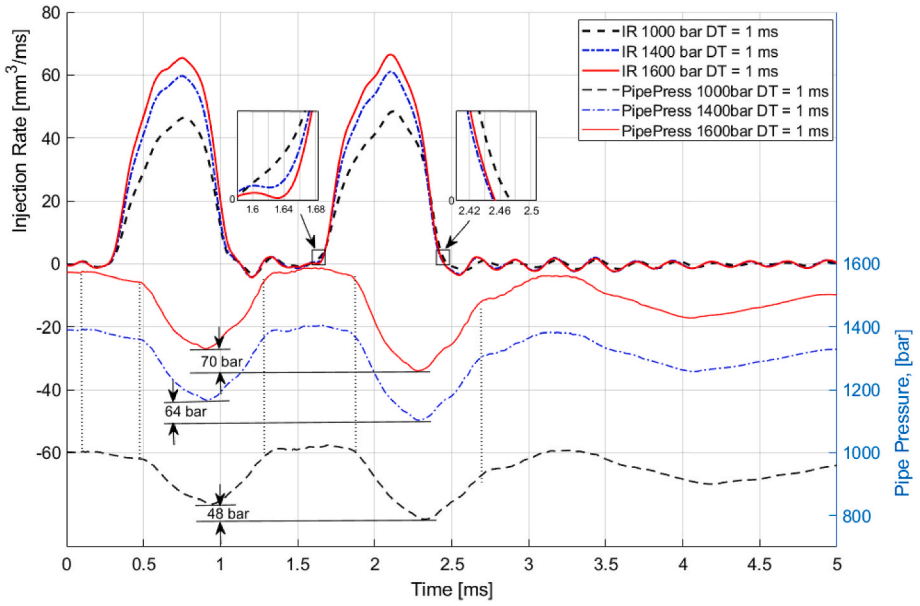

Fig. 13. IR and p_{pipe} of split injection modes under $ET_1 = ET_2 = 0.56$ ms, DT = 1 ms and $\mathbf{p_{rail}}$ **conditions (1000, 1400, and 1600 bar, respectively).**

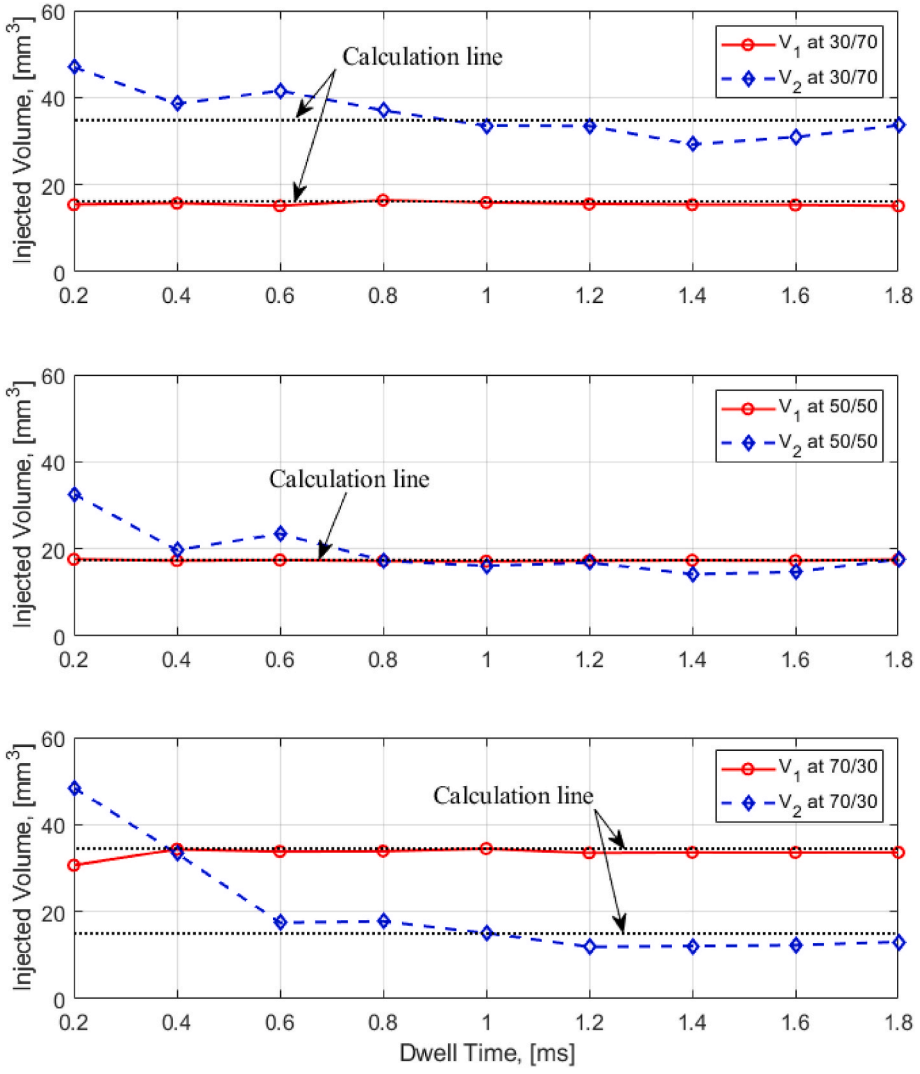

Fig. 14. Total fuel volumes of the first and second shots under $p_{rail} = 1000$ bar, three injection ratios (30/70, 50/50, and 70/30, respectively), and varying DT.

conditions for a single injection, which are systematic. In this work, the inter-cycle instability has been evaluated using the COV, while the deviations are examined through SD of IR. Although the standard deviation of IRs of 300 shots are quite small for both solo and split injection strategies, SD of the split injection modes is slightly bigger than that of single injection modes. The COV of IRs are between 0.5% and 2% for all injection modes, which may imply that the injection process is the main contribution to the compression ignition engine cycle-to-cycle variability.

2. Pipe pressure at SOI of solo injection modes and the first shot of split injection modes is lower than the nominal rail pressure, p_{rail}. Before the injection event, a small amount of fuel is released from the controlling chamber when hole A is opened. An amount of fuel from the pipe is then supplied to the chamber, leading to a pressure drop prior to SOI as mentioned. However, the drop is approximately only 2% of p_{rail}.
3. Similar to common rail multi injection modes, pressure oscillations created by the first shot in the split injection mode have significant effects on IR of the second shot, especially when DT is short (e.g., DT < 0.8 ms in this study). Increasing DT impairs this influence, and the hydraulic behaviors of the second shot are closer to that of the first shot. Correlations between IR of the second shot and different parameters like DT, injection ratio, and pressure conditions may help to adjust the injection parameters to supply fuel in the right time and right amount.
4. Under split injection mode, the time delay between SOE and SOI of the second shot depends on DT and ET. This indicates the influence of pressure oscillation of the first shot to the second shot. Up to a certain DT (e.g., 1 ms in this study), when two shots are far enough from each other, the delay time of the second shot is quite close to that of the first shot.
5. The injection ratio has strong effects on the hydraulic characteristics of the second shot. Bigger fuel amount of the first shot leads to bigger variations in the injection rates of the second shot. Variations in the injection rates of the second shot under the injection ratio of 30/70 is about 6 mm^3/ms (approximately 10.3%), while this value is 16 mm^3/ms (approximately 28%) under the injection ratio of 70/30. This leads to difficulties in controlling the right amount of fuel injected in the second shot.

Globally, the results obtained in the present work evidence how the mutual influences among close-coupled injector actuations add further complexities to the engine management system when utilizing modern injection approaches. The proposed methodology can offer a contribution to the analysis of the actual feasibility of advanced injection strategies for the improvement of combustion control in compression ignition engines.

Author contributions

Conceptualization, methodology, validation, analysis, investigation, and resources: Vu H. Nguyen; Andrea Cavicchi; Dat X. Nguyen; Kien T. Nguyen; Phuong X. Pham and Lucio Postrioti. Writing - original draft preparation: Dat X. Nguyen. Writing - review and editing: Phuong X. Pham, Vu H. Nguyen; Kien T. Nguyen; and Lucio Postrioti. Supervision: Vu H. Nguyen; Phuong X. Pham and Lucio Postrioti. All authors have read and agreed to the published version of the manuscript.

Funding

This research received no external funding.

Declaration of competing interest

The authors declare that they have no known competing financial interests or personal relationships that could have appeared to influence the work reported in this paper.

Acknowledgement

The authors would like to thank Enago (www.enago.com) for the English language review.

References

[1] A. Mulemane, J.-S. Han, P.-H. Lu, S.-J. Yoon, M.-C. Lai, Modeling dynamic behavior of diesel fuel injection systems, SAE Int. J. Engine (2004) 15.
[2] A. Ferrari, A. Mittica, F. Paolicelli, P. Pizzo, Hydraulic characterization of solenoid-actuated injectors for diesel engine common rail systems, Energy Proc. 101 (2016) 878–885.
[3] B.D. Nikolić, K. B, S.D. Marković, M.S. Mitrović, Determining the speed of sound, density and bulk modulus of rapeseed oil, biodiesel and diesel fuel, Therm. Sci. 16 (suppl 2) (2012) 505–514.
[4] L. Postrioti, A. Cavicchi, D. Paolino, C. Guido, M. Parotto, R. Di Gioia, An experimental and numerical analysis of pressure pulsation effects of a Gasoline Direct Injection system, Fuel 173 (2016) 8–28.
[5] R. Mobasheri, Investigations of advanced injection and combustion strategies on DI diesel engine performance and emissions, in: Engineering, University of Sussex, 2012.
[6] K.B. Showry, P.R. Reddy, Reducing Particulate and NOX Emissions by Using Split Injection, Int. J. Sci. Res. 4 (3) (2015).
[7] S. Jafarmadar, The effect of split injection on the combustion and emissions in DI and IDI diesel engines, in: S. Bari (Ed.), Diesel Engine - Combustion, Emissions and Condition Monitoring, InTech, Rijeka, 2013. Ch. 01.
[8] M. Yoon Kim, S. Hyun Yoon, C. Sik Lee, Impact of split injection strategy on the exhaust emissions and soot particulates from a compression ignition engine fueled with neat biodiesel, Energy Fuel. 22 (2008) 1260–1265.
[9] M.R. Herfatmanesh, H. Zhao, Experimental investigation of effects of dwell angle on fuel injection and diesel combustion in a high-speed optical CR diesel engine, in: Proceedings of the Institution of Mechanical Engineers, Part D: Journal of Automobile Engineering, vol. 227, 2012, pp. 246–260.
[10] I.M.R. Fattah, C. Ming, Q.N. Chan, A. Wehrfritz, P.X. Pham, W. Yang, S. Kook, P. R. Medwell, G.H. Yeoh, E.R. Hawkes, A.R. Masri, Spray and Combustion Investigation of Post Injections under Low-Temperature Combustion Conditions with Biodiesel, Energy & Fuels, 2018.
[11] I.R. Fattah, C. Ming, Q. Chan, A. Wehrfritz, P. Pham, W. Yang, S. Kook, P. Medwell, G. Yeoh, E. Hawkes, Spray and combustion investigation of post injections under low-temperature combustion conditions with biodiesel, Energy Fuel. 32 (8) (2018) 8727–8742.
[12] T. Krogerus, K. Huhtala, Diagnostics and identification of injection duration of common rail diesel injectors, Open Eng. 8 (2018) 1–6.
[13] R. Sener, M.U. Yangaz, M.Z. Gul, Effects of injection strategy and combustion chamber modification on a single-cylinder diesel engine, Fuel 266 (2020) 117122.
[14] P.X. Pham, K.T. Nguyen, T.V. Pham, V.H. Nguyen, Biodiesels manufactured from different feedstock: from fuel properties to fuel atomization and evaporation, ACS Omega 5 (33) (2020) 20842–20853.
[15] P. Pham, A. Kourmatzis, S. Khan, A. Masri, Dual-Angle micro-particle tracking velocimetry in the primary atomization zone of electrostatically charged diesel sprays, in: 11th Asia-Pacific Conference on Combustion, 2017.
[16] P. Pham, A. Kourmatzis, A.R. Masri, Simultaneous volume-velocity measurements in the near-field of atomizing sprays, Meas. Sci. Technol. 28 (11) (2017) 115203.
[17] Y. Zhang, T. Ito, K. Nishida, Characterization of mixture formation in split-injection diesel sprays via laser absorption-scattering (LAS) technique, Trans. J. Engine-V110-3 (2001) 14.
[18] A. Cavicchi, L. Postrioti, F.C. Pesce, U. Ferrara, Experimental Analysis of Fuel and Injector Body Temperature Effect on the Hydraulic Behavior of Latest Generation Common Rail Injection Systems, 2018, p. 13. *SAE Technical Paper 2018-01-0282*.
[19] A. Cavicchi, L. Postrioti, F. Berni, S. Fontanesi, R. Di Gioia, Evaluation of hole-specific injection rate based on momentum flux measurement in GDI systems, Fuel 263 (2020) 116657.
[20] L. Postrioti, G. Buitoni, F.C. Pesce, C. Ciaravino, Zeuch method-based injection rate analysis of a common-rail system operated with advanced injection strategies, Fuel 128 (2014) 188–198.
[21] J.B. Heywood, Internal Combustion Engine Fundamentals, McGraw-Hill Education, 2018.
[22] A. Catania, A. Ferrari, M. Manno, E. Spessa, Experimental investigation of dynamics effects on multiple-injection common rail system performance, J. Eng. Gas Turbines Power (2008) 130.
[23] L.A. Catalano, V.A. Tondolo, A. Dadone, Dynamic Rise of Pressure in the Common-rail Fuel Injection System, SAE Technical Paper 2002-01-0210, 2002, https://doi.org/10.4271/2002-01-0210.
[24] A. Catania, A. Ferrari, M. Manno, Development and application of a complete multijet common-rail injection-system mathematical model for hydrodynamic analysis and diagnostics, J. Eng. Gas Turbines Power 130 (6) (2008).
[25] A. Catania, A. Ferrari, E. Spessa, Numerical-Experimental study and solutions to reduce the dwell-time threshold for fusion-free consecutive injections in a multijet solenoid-type CR system, J. Eng. Gas Turbines Power (2009) 131.

[26] C. Arcoumanis, M.S. Baniasad, Analysis of Consecutive Fuel Injection Rate Signals Obtained by the Zeuch and Bosch Methods, SAE Technical Paper 930921, 1993, https://doi.org/10.4271/930921.
[27] W.J.S.T. Bosch, The Fuel Rate Indicator: a New Measuring Instrument for Display of the Characteristics of Individual Injection, 1967, pp. 641–662.
[28] J.M. Desantes, R. Payri, F.J. Salvador, J. Gimeno, Measurements of Spray Momentum for the Study of Cavitation in Diesel Injection Nozzles, SAE International, 2003.
[29] P. Srichai, P.-P. Ewphun, C. Charoenphonphanich, P. Karin, M. Tongroon, N. Chollacoop, Injection Characteristics of Palm Methyl Ester Blended with Diesel Using Zuech's Chamber, Int. J. Automot. Technol. 19 (3) (2018).
[30] J. Li, K. Zhang, Q. Zhang, M. Ouyang, Solenoid Valve Driving Module Design for Electronic Diesel Injection System, 2005, p. 8. *SAE Technical Paper 2005-01-0035*.
[31] L. Postrioti, M. Battistoni, C. Ungaro, A. Mariani, Analysis of diesel spray momentum flux spatial distribution, SAE Int. J. Engines 4 (1) (2011) 720–736, https://doi.org/10.4271/2011-01-0682.